Study of the Pyrolysis of Ayous and Kambala Co-Products: Kinetic Modeling of the Two Species

Mamoun Clévie Aboni Akodzi [1,2], **Pierre Girods [1]**, **Timoléon Andzi-Barhé [2]** and **Yann Rogaume [1,*]**

[1] Université de Lorraine, INRAE, LERMAB, ERBE, F-88000 Epinal, France; pierre.girods@univ-lorraine.fr (P.G.)

[2] Le Laboratoire de Recherche en Chimie Appliquée, Université Marien NGOUABI, Brazzaville 99324, Congo

* Correspondence: yann.rogaume@univ-lorraine.fr

Abstract: A kinetic model based on the two-stage semi-global multi-reaction model of Grioui was developed using the TG and DTG curves for the by-products of Kambala and Ayous. These two tropical species are widely used in the Republic of Congo. The TG and DTG curves were obtained through thermogravimetry at five different heating rates (3, 7, 10, and 20 K/min) up to a final temperature of 800 °C under a nitrogen atmosphere. The thermal decomposition of both species started at similar temperatures, but the profiles exhibited notable differences. Kambala showed a distinct profile with two peaks at approximately 500 °C and 700 °C, which upon further investigation were found to correspond to ash decomposition. Additionally, the shoulder present in Ayous between 250 °C and 300 °C, attributed to hemicelluloses degradation, was absent in the DTG curves for Kambala. The kinetic model for Ayous was formulated in three steps, while the model for Kambala consisted of four steps. Both models accurately predicted the thermal degradation of the wood species, and the resulting kinetic parameters aligned with those reported in the literature.

Keywords: co-products; Congolese wood; ash; modeling; kinetic parameters

1. Introduction

The pressing challenges of greenhouse gas emissions, fossil fuel depletion, and climate change have led mankind to take a step backwards, redirecting its energy decisions toward biomass, which has always been part of our daily lives [1]. Using biomass is beneficial and respectful of the environment, as it reduces certain types of waste (open burning, landfill, etc.) while adding value.

Biomass, which includes materials derived from organic matter such as wood, agricultural byproducts, and waste, plays an important role in reducing environmental pollution, minimizing waste, and providing a renewable source of energy. Among biomass resources, wood is particularly important due to its availability, high-energy potential, and low carbon footprint, making it a key component in the global renewable energy debate. Sub-Saharan Africa, where many countries face electricity shortages, has an abundance of wood waste generated by the growing timber industry [2], This represents a valuable opportunity for energy recovery through the use of wood byproducts such as chips and sawdust, which remain underutilized despite their potential.

In this context, two African wood species, Ayous and Kambala, offer promising potential as biomass fuels due to their availability and wide use across the region.

Chlorophora excelsa, also known as *Milicia regia*, is a member of the Moracea family, commercially referred to Kambala, Iroko, or Mandji in various African countries. This species is a representative of tropical and equatorial forests and is commonly found in regions such as Côte d'Ivoire, Equatorial Guinea, Benin and the countries of the Congo Basin [3].

Ayous, the local name given to *Triplochiton scleroxylon* in Cameroon, Gabon, and Congo Brazzaville. It belongs to the Malvaceae family. It is classified as a whitewood or secondary

wood. Despite being classified as a white wood, the Ayous species displays good physical, mechanical, and durability properties [4].

The availability and wide use of these wood species (commercial, cultural, medicinal, construction, etc.) means that there is a large production of by-products (chips and sawdust), which unfortunately have no outlet.

Thermochemical processes like pyrolysis, combustion, and gasification have emerged as key methods for converting biomass into usable energy. Among these, pyrolysis stands out both as a stand-alone process and as a precursor for other thermochemical transformations. However, further research is needed to improve our understanding of these processes and to optimize their implementation [5,6].

The study of wood decomposition kinetics is fundamental to any study of thermal recovery, as it describes the overall behavior of wood at specific temperatures (high and low) [7]. Hence the great interest among scientists, with a variety of works in the literature having different kinetic models with the sole aim of understanding the degradation process of wood material [8–11]. Prakash et al. [12] and Di Blasi et al. [13] summarized several models which have been studied in recent years. Three models stand out from these studies.

A one-stage global model: This is the first approach to modeling wood pyrolysis. This model represented in the Figure 1, treats pyrolysis as a reaction of the first order, with the solid breaking down into volatile gas and charcoal [14,15]. This model is empirical and does not represent real-life situations, and hence its rarity in the literature [12].

Figure 1. Overall one-step mechanism.

A one-step multi-global model: As illustrated in Figure 2, in this model, secondary reactions are grouped with primary reactions. Since the model has been delimited by the primary kinetic parameters, the char yield is variable [16,17].
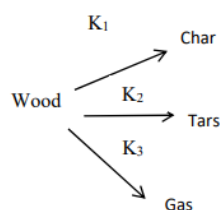
Figure 2. Multi-global mechanism in one step.

A semi-global model with two or more stages: As shown in the Figure 3, this model takes into account the primary and secondary stages and expresses the kinetic data for each, unlike the single-stage model. Several authors in the literature have developed multi-reaction models to explain the degradation of wood and its constituents, including Goldstein [8], Shafizadeh [18], Chan et al. [19], and Di Blasi et al. [20]. This model is more widely accepted in the literature than the first two, with kinetic parameters frequently used in the literature.
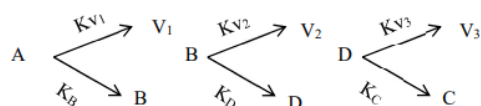
Figure 3. A multi-stage, multi-global mechanism.

Two major contradictory ideas have emerged from the large number of kinetic models in the literature. The first is that wood is a homogeneous material and therefore behaves thermally like the sum of its three main compounds—hemicellulose, cellulose,

and lignin [21,22]—analyzed separately. For the second, the decomposition of wood is modeled to be consistent with the degradation of these three constituents. Consequently, the degradation of wood is much more complex since several aspects need to be taken into account [3,9,23]. The first approach is widely used in the literature, with the majority of wood modeling studies incorporating this approach, although the interactions between these three compounds and the effects of minerals present in the wood are not taken into account.

The model proposed by Grioui et al. [9] is a two-stage, semi-global, multi-reaction kinetic model based on the fact that the thermal behavior of wood is different from that of the three main compounds, which are analyzed separately after the conclusion of a study on the carbonization of olivine wood. This model divides wood into three pseudo-solids (A_1, A_2, and A_3, which are not considered to correspond to hemicelluloses, cellulose, or lignin), with each solid corresponding to a mass fraction α_1, α_2, and α_3, respectively. The solids A_1 and A_2 degrade completely to produce gas (G_1 and G_2, respectively) and a non-degradable residue C_2, considered char. The last solid A_3 degrades into gas (G_3) and an intermediate component B, which in turn degrades into gas (G_4) and a non-degradable solid residue C_3, assumed to also be char. The four reactions are governed by the law of the first order. The rate constants obey Arrhenius's law. The masses of the products from the reactions in Equations (2), (3), and (4) are denoted as mC_2, mB and mC_3, respectively.

The rate constants obey Arrhenius' law.

$$A_1 \xrightarrow{K_1} G_1(Gas) \tag{1}$$

$$A_2 \xrightarrow{K_2} \gamma_2 C_2(Coal) + G_2 \ (Gas) \tag{2}$$

$$A_3 \xrightarrow{K_3} \beta B(Intermediary \ solid) + G_3 \ (Gas) \tag{3}$$

$$B \xrightarrow{K_4} \gamma_3 C_3(Coal) + G_4 \ (Gas) \tag{4}$$
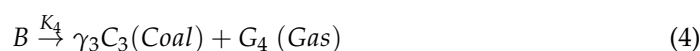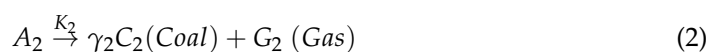
The aim of this study is to develop a multi-reaction kinetic model for the pyrolysis of Ayous and Kambala based on the model approach of Grioui et al. [9]. Pyrolysis behavior up to 800 °C is studied using isothermal and dynamic thermogravimetry at different heating rates, which is an original approach; no data are currently available concerning the two wood species studied in this article. Moreover, in several previous works in the literature, it has been observed that most models treat wood as a homogeneous material without taking into account the interactions between its components or the influence of minerals which are present in relatively high percentages in tropical wood species. Particular emphasis is placed on the high-temperature behavior of Kambala, which exhibits non-standard thermal degradation due to its mineral content. This work contributes to the field of biomass energy by providing new information on the pyrolysis mechanisms of these African woods, which can serve as models for other tropical species. Finally, these data will be useful for the development and global modelization of processes which could be further developed for wood waste energy valorization, such as carbonization, combustion, or gasification, in order to reach two parallel objectives: find an outlet for this waste which is available in large quantities and solve the problem of recurring electricity shortages in African countries.

2. Materials and Methods

2.1. Raw Material Collection and Preparation

The two biomass samples tested in this work, Ayous and Kambala, are by-products of tropical wood species harvested from a sawmill in the fourth arrondissement of the Republic of Congo. The materials were initially ground using a cutting mill (Cutting Mill SM 100, Retsch, Haan, Germany) and further crushed into powder with a ball mill (Cryomill, Retsch) to obtain homogeneous samples. Then, the wood powder was oven-dried (103 °C) for 48 h.

2.2. Thermogravimetric Analysis (TGA)

The mass loss of the Kambala and Ayous by-products was measured using a NET-ZSCH STA 449 F3 Jupiter thermobalance, NETZSCH-Gerätebau GmbH, Selb, Germany. For each sample, 50 mg of powder was placed in a platinum crucible. Triplicate tests were carried out under an inert nitrogen atmosphere at different heating rates (3, 5, 7, 10 and 20 K/min), with the temperature rising from 25 °C to 800 °C. The dynamic phase was followed by a 1 h isothermal phase to ensure that the residual solid mass remained approximately constant. A blank run was performed prior to each analysis at all selected heating rates to eliminate potential interference.

2.3. Ash Effect Higlights

To confirm that the peaks observed at 500 °C and 700 CorrespondenceC on the curves obtained from the TGA during the pyrolysis of Kambala were a result of ash, two modifications were made to the Kambala powder sample, and new TGA tests were conducted on the modified Kambala.

The first approach involved demineralizing the Kambala sample using accelerated solvent extraction (ASE) (3 cycles at 80 °C under 10 bars). After extraction, the powder was dried in an oven for 48 h. A portion of the sample (2 g) was analyzed using X-ray fluorescence spectroscopy (XRF) to compare the raw material with the demineralized sample and assess the efficiency of the demineralization by examining various metal contents.

The second approach was to artificially increase the ash content of the Kambala sample by adding ash. The ash was generated during ash content measurement in a muffle furnace at 815 °C. Based on the known ash content of the raw Kambala, the mass of additional ash was calculated to achieve a total ash content of 10 wt%.

Complementary analyses were performed on the ash using TGA, coupled with gas analysis via µGC-TCD (R3000, SRA instrumentation, l'Etoile, France, molsieve 5A column) for ash thermal behavior investigations.

2.4. Kinetic Modeling

As outlined in the introduction, the kinectic model used in this study is based on the multi-reaction model proposed by Grioui et al. [9]. Because of differences in observed the thermal behavior of Kambala and Ayous, which are discussed in Results and Discussion, the considered degradation mechanisms taking kinetic studies into account were different. For Kambala, a four step mechanism was considered, but for Ayous, the mechanism was in three steps.

The used kinetic models for this article were as follows:

Reaction n°	Kambala	Ayous
1	$A_1 \rightarrow G_1(gas)$	$A_1 \rightarrow G_1(gas)$
2	$A_2 \rightarrow Y_2 C_2(char) + G_2(gas)$	$A_2 \rightarrow Y_2 C_2(char) + G_2(gas)$
3	$A_3 \rightarrow \beta B$ *(intermediate solid)* + $G_3(Gas)$	$A_3 \rightarrow Y_3 C_3(Char) + G_3(gas)$
4	$B \rightarrow Y_3 C_3(Char) + G_4(gas)$	

For Kambala, the first two pseudo-solids, A_1 and A_2, degrade in a simple reaction which produces gases G_1 and G_2 for the reactions 1 and 2 and a non-degradable solid residue C_2, considered as char, for reaction 2. For A_3, the degradation mechanism is in two steps in series. A_3 degradation (reaction 3) produces an intermediate solid B and a gas G_3. In a second trial (reaction 4), B is transformed into a non-degradable solid residue C_3 and a gas G_4.

For Ayous, the three pseudo-solids A_1, A_2, and A_3 degrade in a simple reaction which produces gases G_1, G_2, and G_3, for the reactions 1, 2, and 3, and the non-degradable solid residues C_2 and C_3 are considered as char for the reactions 2 and 3.

By assuming that the kinetics are described by first-order laws for all reactions, the mass balance of these different solids for Kambala can be written as follows:

$$\frac{dm_{A1}}{dt} = -k_1 m_{A1} \tag{5}$$

$$\frac{dm_{A2}}{dt} = -k_2 m_{A2} \tag{6}$$

$$\frac{dm_{A3}}{dt} = -k_3\, m_{A3} \tag{7}$$

$$\frac{dm_{C2}}{dt} = \gamma_2 k_2 m_{A2} \tag{8}$$

$$\frac{dm_B}{dt} = \beta k_3\, m_{A3} - k_4 m_B \tag{9}$$

$$\frac{dm_{C3}}{dt} = \gamma_3 k_4 m_B \tag{10}$$

where k_1, k_2, k_3, and k_4 are the rate constants of the reactions in Equations (5 to 10), and mA_1, mA_2, mA_3, mC_2, mB, and mC_3 represent the mass of the constituents A_1, A_2, A_3, C_2, B, and C_3, respectively. Here, $m(t)$ represents the total mass of the sample at the time t, which is the sum of the mass of the different solids:

$$m(t) = m_{A_1}(t) + m_{A_2}(t) + m_{A_3}(t) + m_{C2}(t) + m_B(t) + m_{C3}(t) \tag{11}$$

The values of k_i are calculated following Arrhenius's law:

$$k_i = k_{0i} * Exp\left(-Eai/R * T\right) \tag{12}$$

where k_i (s^{-1}) is the rate constant of reaction (i), k_{0i} is the pre-exponential factor, Eai is the activation energy (kJ/mol), R (J/mol.K) is the perfect gas constant, and T is the reaction temperature, expressed in kelvin (K).

For Ayous, the mass balance is written as follows:

$$\frac{dm_{A1}}{dt} = -k_1 m_{A1} \tag{13}$$

$$\frac{dm_{A2}}{dt} = -k_2 m_{A2} \tag{14}$$

$$\frac{dm_{A3}}{dt} = -k_3\, m_{A3} \tag{15}$$

$$\frac{dm_{C2}}{dt} = \gamma_2 k_2 m_{A2} \tag{16}$$

$$\frac{dm_{C3}}{dt} = \gamma_3 k_3\, m_{A3} \tag{17}$$

The total sample mass at time t is the sum of the masses of the different solids:

$$m(t) = m_{A_1}(t) + m_{A_2}(t) + m_{A_3}(t) + m_{C2}(t) + m_{C3}(t) \tag{18}$$

In the work of Griou et al., the system of differential equations was solved analytically while considering constant k_i values throughout the experiments, which were carried out under isothermal conditions at different temperatures. In the present study, the experiments were carried out under dynamic and isothermal conditions, which made the mathematical solution of the differential equations more complex. Consequently, a numerical alternative method was used to solve the system based on the following equations:

$$m_i(n+1) = m_i(n) + {dm_i(n)}/{dt} * \Delta t, \text{ with } \Delta t \text{ as the sampling time and } \Delta t = 0.1 \text{ min}$$

The initial conditions were as follows:

$$m_{A_1}(0) = \alpha_1 \; ; \; m_{A_2}(0) = \alpha_2 \; ; \; m_{A_3}(0) = \alpha_3 \; ; \; m_B(0) = m_{C2}(0) = m_{C3}(0) = 0$$

For each experimental condition, an error function (sum of the squared difference between the calculated and experimental values of the mass) was calculated. Then, the values of the different kinetic parameters were optimized by minimizing the error function.

3. Results and Discussion

3.1. Characterization of Wood Species

Tables 1 and 2 below present the characterization results of Kambala and Ayous.

Table 1. Chemical composition of Kambala.

Ultimate Analysis	Percent (%)	Metals	Percent (mg/kg Dry)
Carbon	51.7	Aluminum	23
Hydrogen	4.9	Calcium	9945
Nitrogen	0.2	Iron	26
Oxygen	43.5	Magnesium	595
Fluorine	<20	Phosphorus	<15
Sulphur	109	Potassium	3604
Chlorine	<70	Sodium	12
Silica	294		
Ash	3.6		

Table 2. Chemical composition of Ayous.

Ultimate Analysis	Percent (%)	Metals	Percent (mg/kg Dry)
Carbon	51.4	Aluminum	47
Hydrogen	5.7	Calcium	5899
Nitrogen	0.5	Iron	60
Oxygen	42.4	Magnesium	278
Fluorine	<20	Phosphorus	49
Sulphur	1117	Potassium	773
Chlorine	469	Sodium	14
Silica	153		
Ash	1.9		

The elemental analysis (NF EN ISO 29541 standard method) [24] and metal content quantification (NF EN ISO 11885) [25] were conducted by an external private laboratory following European standards.

The ash content was determined by combustion at 815 °C in a muffle furnace.

The chemical composition of the wood samples was consistent with the values reported in the literature [5,26].

According to the results of the elemental analyses, the chemical formula of Kambala is $CHO_{0.65}$.

According to the results of the elemental analyses, the chemical formula of Ayous is $CH_{1.4}O_{0.64}$.

3.2. Thermogravimetric Analysis of Two Types of Wood

Figures 4 and 5 present the mass loss curves (TG) and their derivative curves (DTG) under nitrogen at different selected heating rates (3, 5, 7, 10, and 20 K/min) for Ayous and Kambala.
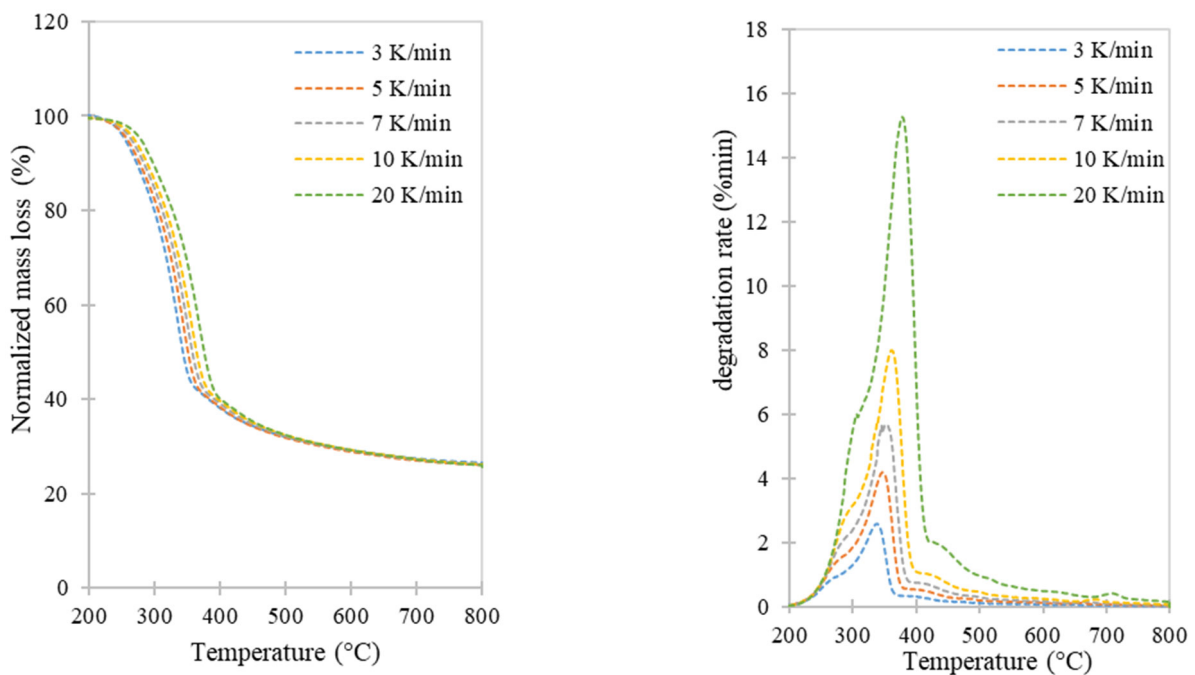
Figure 4. Mass losses (TG) and derivatives (DTG) of the Ayous for the four heating speeds.
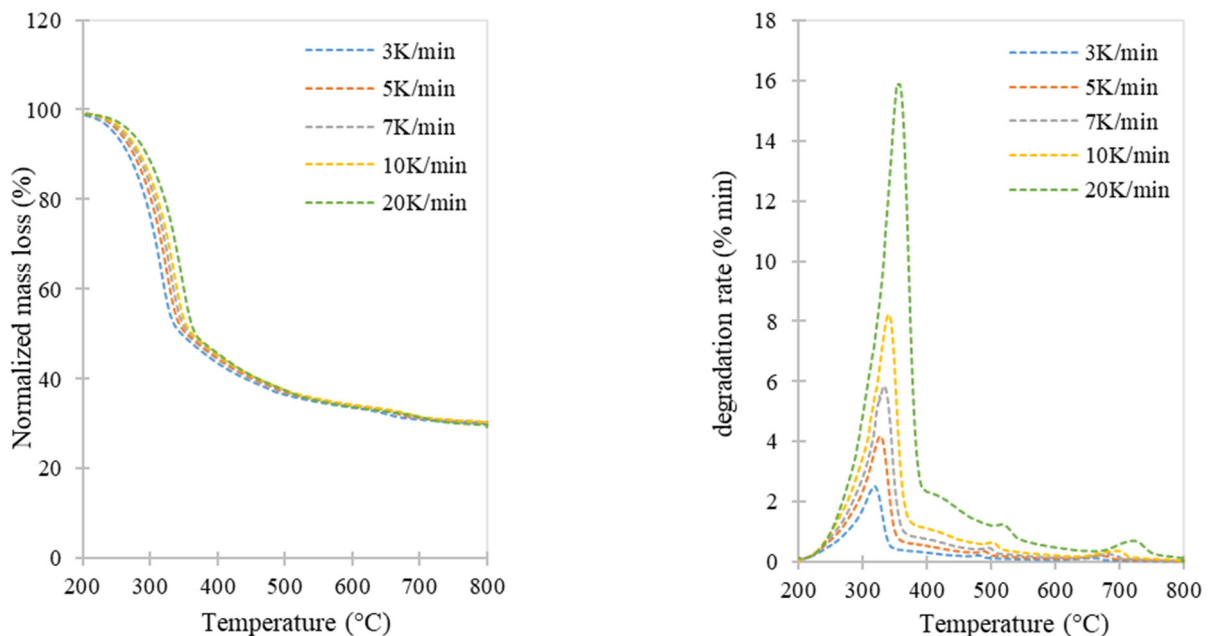
Figure 5. Mass losses (TG) and derivatives (DTG) of Kambala for the four heating speeds.

Detailed analysis of the TG and DTG curves is presented in Table 3.

The TG curves for both species were similar across all heating rates, showing no significant mass loss up to 200 °C due to the prior drying of the samples, which eliminated the moisture region. The major information which can be obtained by observation of the TG curves is the final residual mass percentage after the plateau at 800 °C. Even if the effect is hardly observable on the TG curve, the values of the residual mass percentage given in Table 3 show an effect from the heating rate. In order to highlight this, Figure 6 below gives the evolution of the value of this criteria for both wood species as a function of the heating rate.

Table 3. TGA and DTG analysis and comparison.

Wood Species	Heating Rate	Residual Mass Percent	Begin the First Peak	Shoulder	Maximum Degradation Rate for the First Peak	End of the First Peak	Begin Second Peak	Maximum Degradation Rate Second Peak	End of the Second Peak	Begin Thrid Peak	Maximum Degradation Rate Third Peak	End Third Peak
	3	26.4	178	269	339.9	374.4	-	-	-	-	-	-
	5	25.97	180	280	349.4	385	-	-	-	-	-	-
Ayous	7	25.99	190	289	353.8	391.7	-	-	-	-	-	-
	10	25.86	197	299	364	405.8	-	-	-	-	-	-
	20	25.49	214	309.2	380	426.8	-	-	-	-	-	-
	3	29.77	175	-	319	355.8	463.2	484	498	611	657.3	676.8
	5	30.21	181.3	-	329	365	475.4	490.3	502.4	623.9	674.4	701
Kambala	7	30.08	188.5	-	331.5	368	477.7	495	509	640	681.5	707
	10	29.96	191	-	341.9	381.8	486.8	503.8	516.8	656	697.8	715.8
	20	29.3	205	-	357	396.7	494.7	520.7	542	675	722.6	752.6
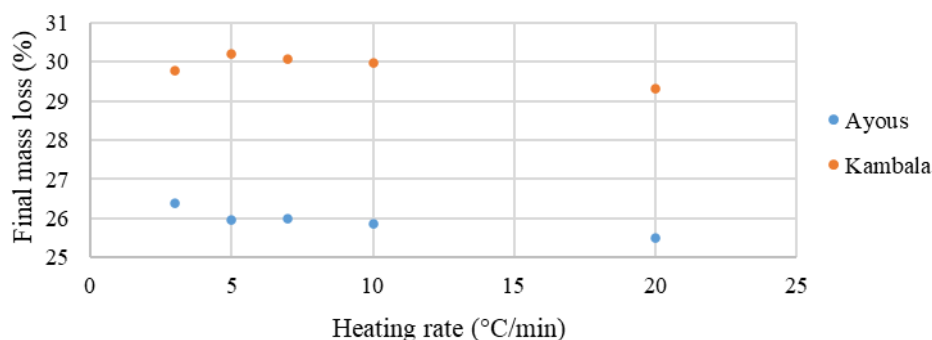
Figure 6. Evolution of residual mass percentage as a function of heating rate for Ayous and Kambala.

Whatever the biomass type, the higher the heating rate, the lower the residual mass yield was. This effect has been described in the literature [27–31]. Different theories have been given to explain this phenomenon.

Haykiri-Acma et al. [28] studied rapeseed's slow pyrolysis. The effect of the heating rate on the char yield was attributed to the reactions of polymerization and condensation of radical components occurring during pyrolysis, deemed responsible for the formation of char. Lower heating rates slowed down the reaction rates and made the residence time of volatiles in the carbon matrix along the pyrolysis process longer. This therefore favors secondary reactions, namely cracking, repolymerization, and recondensation, which promote char production.

Li et al. [29], who worked on the slow pyrolysis of pinewood, showed the same effect and summarized the works of Collard et al. [30] and of Williams et al. [31] to explain the decrease in residual mass with the heating rate.

Collard et al. [30] explained that different types of chemical bonds exist in wood which are more or less sensitive to thermal degradation. With a low heating rate, the weakest bonds break easily, while the stronger bonds remain stable. The polymer's structure is therefore affected slightly, which leads to rearrangement reactions, and the stable carbon matrix would inhibit the release of volatiles, causing a higher yield of bio-char.

Williams et al. [31] showed that at a higher heating rate, more bonds break before the rearrangement reactions happen, resulting in a more compact structure for the char, which delays the heat transfer. In these conditions, the heating rates of the biomass are lower than the set values. Hence, the char yield rate increases.

The residual mass yield after the plateau at 800 °C was higher for Kambala (approximately 30%) than for Ayous (approximately 25%). This point may be attributed to the higher ash content in Kambala. According to Puri et al. [32], alkali metals such as potassium, calcium, and magnesium tend to promote char yield in pyrolysis conditions. Their contents in Kambala are mostly higher than those of Ayous (i.e., Tables 1 and 2), which could therefore explain this result. Moreover, knowing the thermal stability of ash at high

temperatures, the higher the ash content, the higher the residual mass is after pyrolysis. This point was confirmed in this work through comparison of the thermal behavior of raw and ash-enriched Kambala (i.e., Section 3.3.2).

For a better comparison of the thermal behavior of Ayous and Kambala, Figure 7 illustrates the DTG curves between 200 and 500 °C for the 5, 10, and 20 K/min tests.
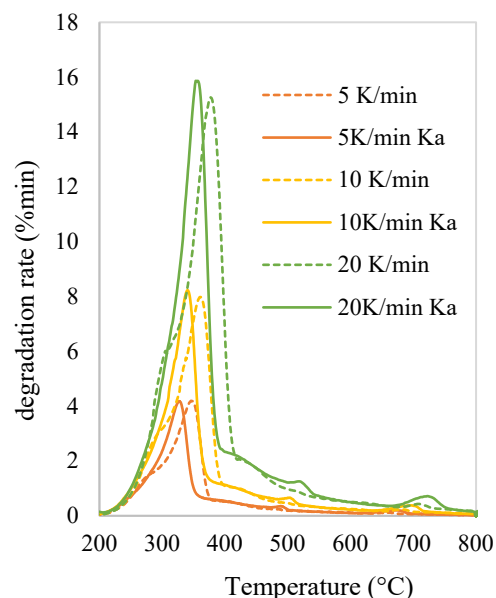
Figure 7. Comparison of DTG curves for Kambala (Ka) and Ayous in the range of 200–800 °C for 5, 10, and 20 K/min.

The DTG curves, however, reveal distinct differences in the pyrolysis behavior of the two species, despite the main degradation occurring between 250 °C and 400 °C for both. Ayous showed a shoulder between 250 °C and 300 °C, which was absent in Kambala. This shoulder is typically attributed to the degradation of hemicelluloses, which decompose at lower temperatures than cellulose. In the case of Kambala, the degradation of cellulose completely overlaps that of hemicelluloses, making the shoulder invisible. The maximum rate of degradation for the cellulose degradation peak reached between 340 °C and 380 °C for Ayous and between 320 °C and 357 °C for Kambala.

The peak for lignin degradation does not appear distinctly in the DTG curves because lignin degrades gradually over a broader temperature range which overlaps with cellulose and hemicelluloses degradation [13,23,33].

In Kambala, two additional peaks can be observed near 500 °C and 700 °C, suggesting further degradation. Due to Kambala's higher ash content, further tests were carried out to determine the influence of ash on pyrolysis and whether these peaks were related to the presence of mineral salts in the ash.

The temperature ranges and maximum degradation rate temperatures for each peak and for both biomasses are detailed in Table 3. It can be observed in Figure 7 and in Table 3 that the increase in the heating rate resulted in the peaks shifting toward higher temperatures. To highlight this point, see Figure 8 below.

This phenomenon is classically described in the literature and is attributed to problems with heat transfer limitations, leading to temperature gradients in samples [23]. Indeed, in the TGA device, the sample temperature is measured at the surface of the sample, which is necessarily higher than that at the core, meaning that the measured temperature is always slightly overestimated. The temperature gradient increased for higher heating rates, explaining the shift to higher temperatures observed while increasing the heating rate.
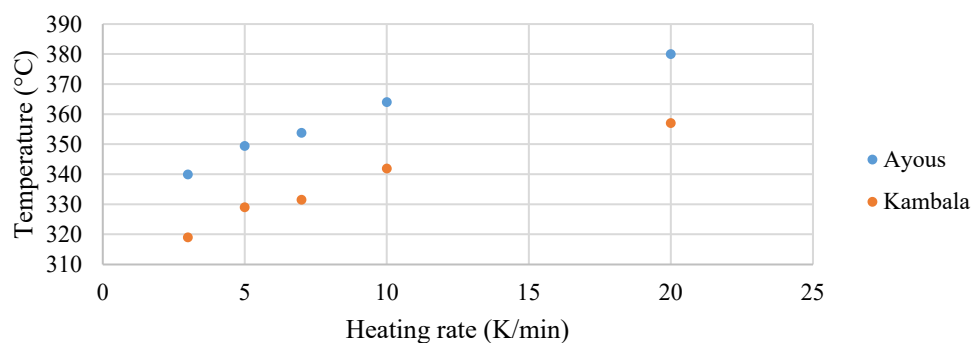
Figure 8. Evolution of maximum degradation rate temperature for the first peak as a function of the heating rate for Ayous and Kambala.

It was also observed that Kambala tended to degrade at lower temperatures than Ayous. Specifically, the highest peak in the Kambala DTG curve at a heating rate of 20 K/min occurred at approximately 357 °C, whereas the peak for Ayous was higher at approximately 380 °C. This behavior suggests that certain minerals present in the ash of Kambala contribute to its accelerated thermal degradation, making it more sensitive to heat compared with Ayous. Puri et al. [32] confirmed this hypothesis in their studies. They showed that specific components of ash influence the thermal degradation pathway of biomass. These components can act either as catalysts, accelerating the thermal degradation process, or as inhibitors, slowing it down. The effect depends on the composition and reactivity of the minerals present in the ash, such as alkali and alkaline earth metals. This interaction highlights the complex role of ash in modifying the thermal stability and breakdown of biomass materials.

3.3. Highlighting Ash's Effect

3.3.1. Effect of Demineralization

The Kambala sample was demineralized by washing it with distilled water using the accelerated solvent extraction (ASE) method. The metal content in both the untreated and demineralization samples was analyzed using XRF, with the results presented in Figure 9. The analysis revealed a significant reduction in the potassium content, with the peak intensity reduced by a factor of three. This reduction was likely due to the removal of monovalent alkali metals, such as potassium [22], during the washing process, which caused the cell walls of the biomass to disintegrate into fibers. This finding aligns with the work of Deng et al. [34], who demonstrated that water washing significantly reduces the yield and proportion of potassium released in gaseous species during biomass degradation.

A comparison of the thermal behavior (TG and DTG) of the two Kambala samples (raw and demineralized), illustrated in Figure 10, reveals a slight shift in the maximum degradation peak (DTG) toward the higher temperatures for the demineralized sample. This shift can be attributed to the catalytic effect of potassium. In the demineralized sample, where the potassium content was significantly reduced, the degradation process was delayed. However, potassium reduction alone does not fully account for this shift. The washing process with distilled water likely removed some extractives, contributing to the observed variations in thermal behavior. It is noteworthy that no significant differences were observed in the peaks at 500 °C and 700 °C.

Nowakowski et al. [35] also reported a shift toward higher temperatures in their study on potassium's catalytic role in the pyrolysis of short- rotation coppice willow. They concluded that the shift resulted from the removal of certain catalytic species, consistent with our observations. For clarity, the TG and DTG curves for the three heating rates, rather than all five, are presented for improved visibility.
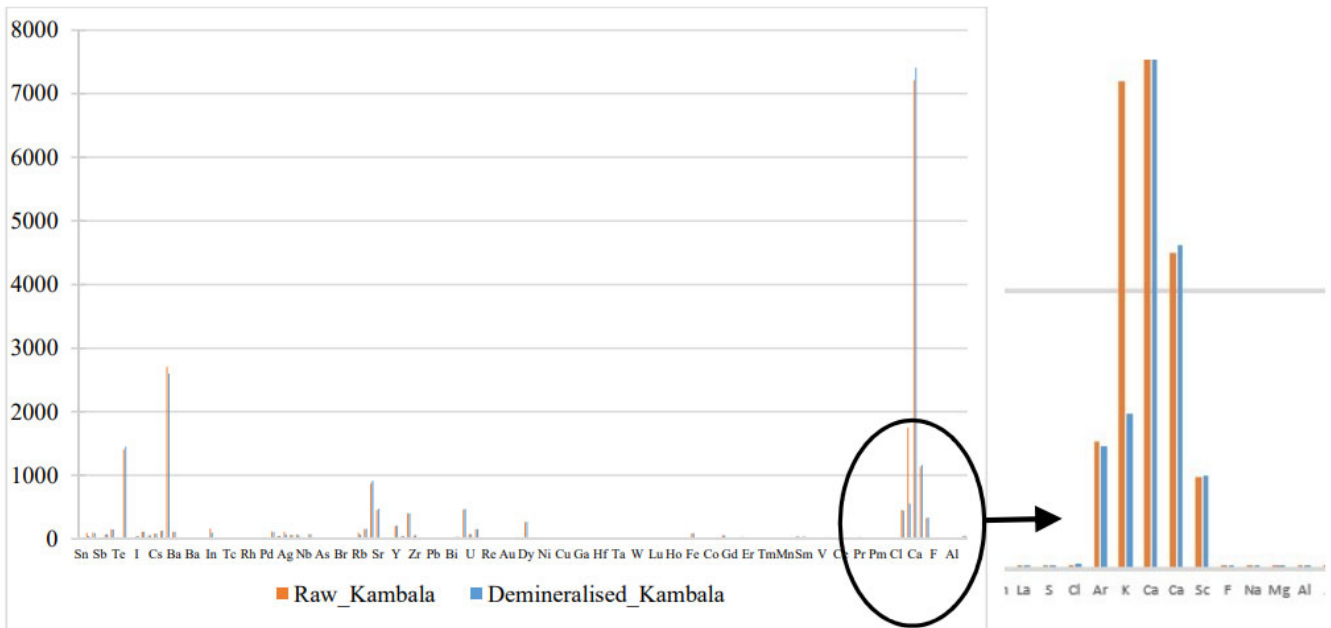
Figure 9. Comparison of metal content in Kambala samples before and after demineralization.
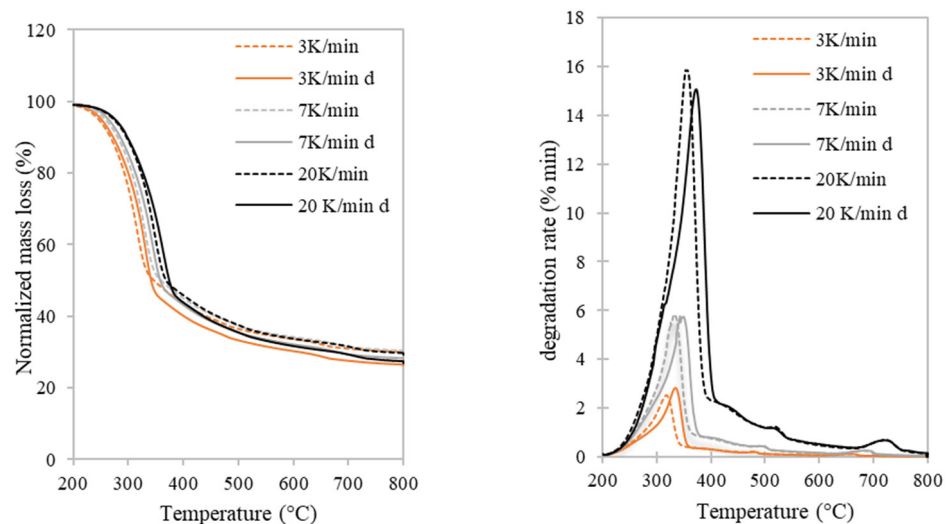
Figure 10. Comparison of mass loss curves (TG) and derived mass loss curves (DTG) for Kambala before and after demineralization.

The demineralization of the Kambala sample had no significant impact on the two peaks observed at approximately 500 °C and 700 °C. This outcome was anticipated, given the limited efficiency of the demineralization process. The persistence of these peaks suggests that the minerals responsible for these thermal events were not effectively removed during the demineralization step.

3.3.2. Effect of Ash Enrichment

The demineralization was reversed by blending the Kambala powder (mb = 9.38 g) with Kambala ash (mC = 0.62 g), which was obtained after combustion at 815 °C in a muffle furnace. This procedure increased the ash content from 4% to 10%. A TGA test was then performed on the ash-enriched sample at a heating rate of 20 K/min. As shown in Figure 11, the peak observed near 700 °C became significantly more pronounced in the DTG curve of the mineral-enriched sample. This suggests a clear correlation between the

ash content and the observed thermal behavior. A preliminary interpretation is that this phenomenon could be attributed to the catalytic effect of ash on pyrolysis char at high temperatures. However, a comparison of the TG curves reveals a slower degradation rate (with a higher residual mass post pyrolysis) for the ash-enriched sample compared with the raw material. This last observation contradicts the initial hypothesis of a catalytic effect, which would typically enhance the degradation.
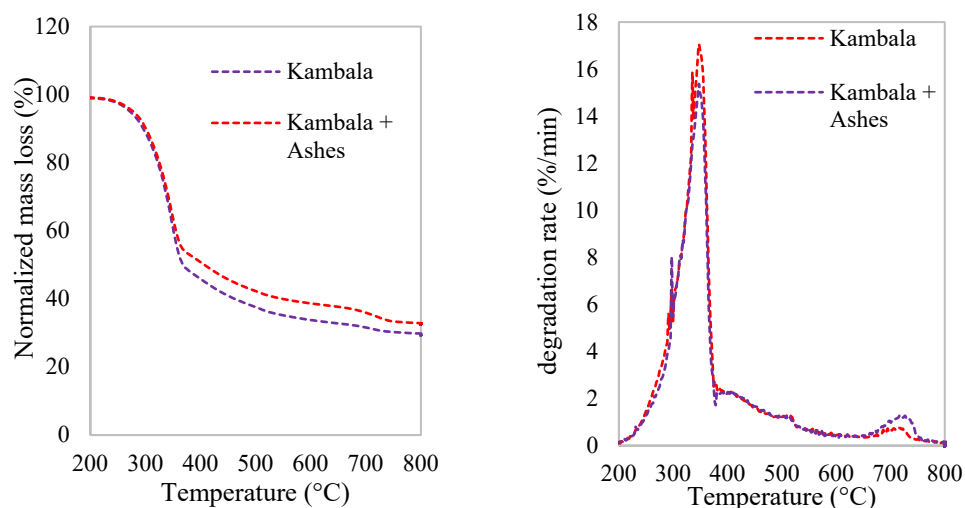
Figure 11. Mass losses (TG) and derivatives (DTG) of Kambala + ash at 20 K/min.

To gain further insight into this phenomenon, the TG curves were recalculated on a dry ash-free (DAF) basis, thereby isolating the degradation of the wood mass from the influence of ash. The TG and DTG curves in Figure 12 show no significant difference in the thermal behavior of the organic matter between the parts of the samples, indicating the ash did not exert a catalytic effect on char degradation.
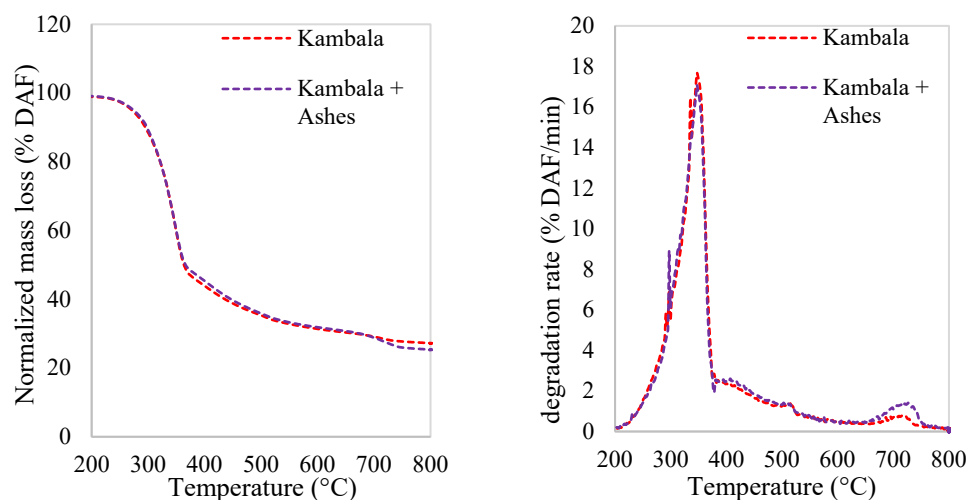
Figure 12. Comparison of the TG and DTG curves (expressed on a DAF basis) for raw and ash-enriched Kambala (temperature rise rate of 20 K/min).

Based on this, we conclude that the peak observed near 700 °C was not related to char degradation but rather to the volatilization of ash components at elevated temperatures. This interpretation also explains the higher residual mass observed for the ash-enriched sample in Figure 11, as an increased ash content results in less organic matter available for degradation.

To confirm this last assumption, the thermal behavior of the ash alone was studied via TGA at a temperature rise rate of 20 K/min, as shown in Figure 13.
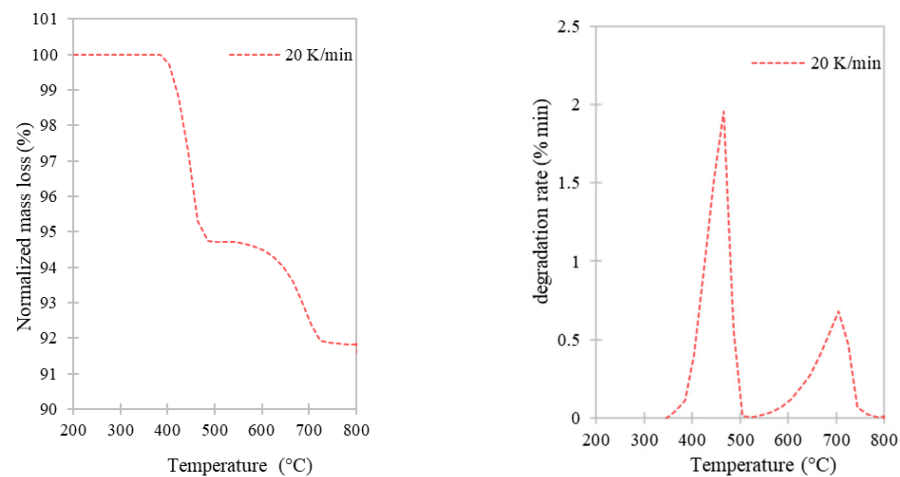
Figure 13. Mass loss (TG) and derivatives (DTG) of Kambala ash at 20 K/min as a function of temperature.

It is evident that the ash exhibited two major degradation peaks near 500 °C and 700°C, confirming that at these temperatures, only the ash underwent degradation. On-line gas composition monitoring at the TGA outlet, conducted via micro gas chromatography (μGC), detected emissions of CO_2 and, to a lesser extent, O_2 during high-temperature degradation of the ash (second peak). These emissions are indicative of decarburization and deoxidation reactions.

3.4. Kinectic Modeling

Figures 14 and 15 compare the experimental results for Kambala and Ayous with the model predictions. The model showed a reasonably good fit with the experimental data across the five selected heating rates curves and the model for the five selected heating speeds. However, a discrepancy was observed in the temperature range of 400–600 °C for all heating rates, which may be attributed to the relatively high ash content in these wood species.

The developed model was used to optimize the kinetic parameters presented in Tables 4 and 5. These parameters were obtained through simulation using Excel software, version 2016. The results were satisfactory when compared to the model, considering key factors such as temperature variation, the heating rate, and the relatively high percentage of mineral elements. The values of the error function (dimensionless) are given in Table 6.

Table 4. Kinetic parameters of Kambala.

Reaction	E_{ai} $(Kj.mol^{-1})$	k_{0i} (s^{-1})	α_i	γ_2	β	γ_3
1	1.24×10^2	6.00×10^9	0.10	-	-	-
2	7.51×10^1	8.11×10^2	0.24	0.42	-	-
3	1.56×10^2	2.00×10^{11}	0.66	-	0.39	-
4	1.70×10^2	1.00×10^7	-	-	-	0.78

Table 5. Kinetic parameters of Ayous.

Reaction	E_{ai} $(Kj.mol^{-1})$	k_{0i} (s^{-1})	α_i	γ_2	γ_3
1	1.30×10^2	6.00×10^9	0.17	-	-
2	8.77×10^1	7.99×10^2	0.26	0.21	-
3	1.62×10^2	2.07×10^2	0.57	-	0.57
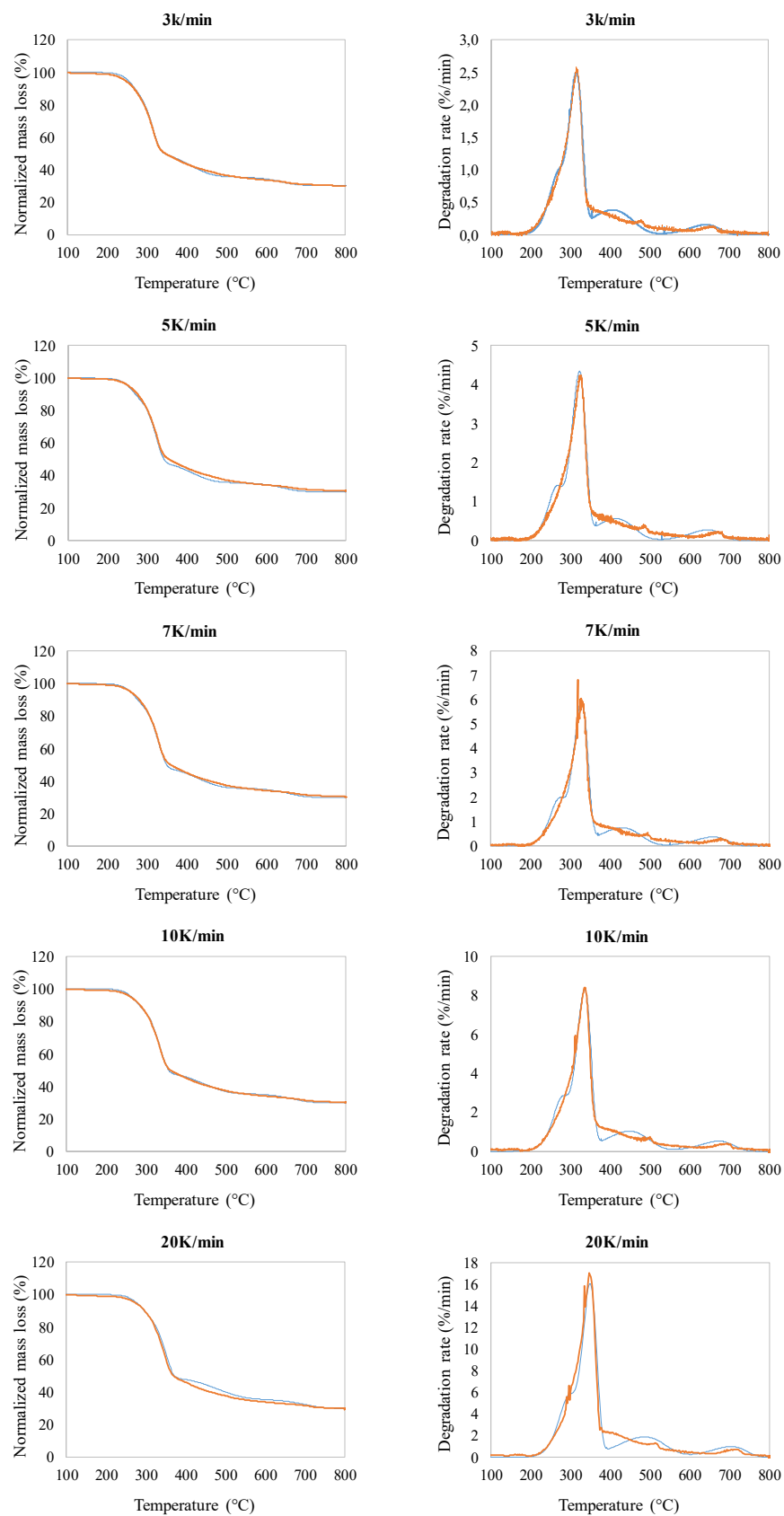
Figure 14. Experimental curves for Kambala compared with the model with five heating speeds.
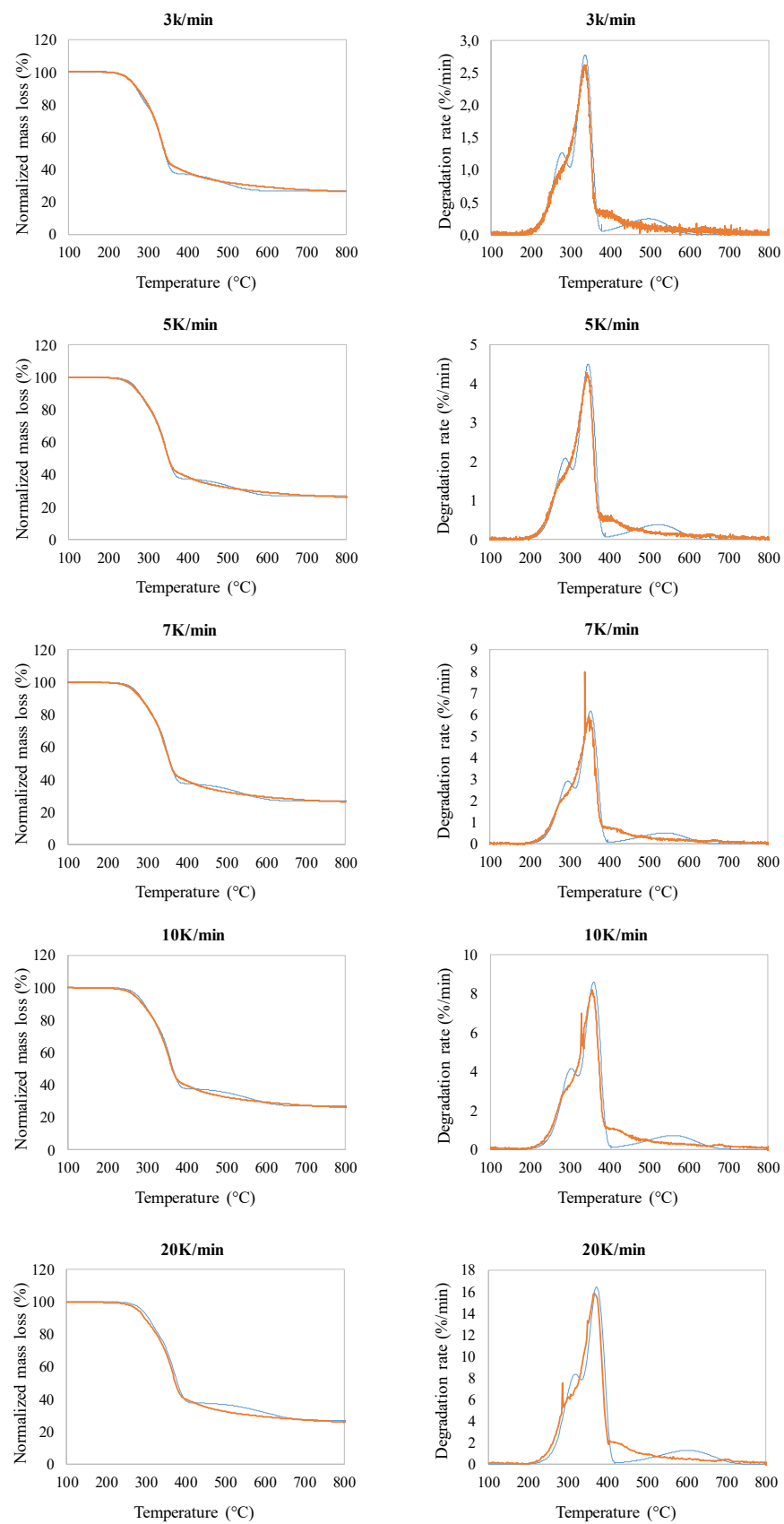
Figure 15. Experimental curves for Ayous compared with the model with five heating speeds.

Table 6. Values of error function for different conditons after kinetic parameter optimization.

Wood Species	Heating Rate	Error Function
	3	0.439
	5	0.154
Ayous	7	0.139
	10	0.145
	20	0.221
	3	0.131
	5	0.223
Kambala	7	0.072
	10	0.028
	20	0.101

The various parameters involved in the kinetic model (α_1, α_2, α_3, Ea_1, Ea_2, Ea_3, Ea_4, k_{01}, k_{02}, k_{03}, k_{04}, γ_2, γ_3, and β) could not be directly measured or experimentally determined. Instead, they were derived from the data set which best fit all of the TG and DTG curves at the chosen heating rates. The parameters from Grioui's model were used as initial estimates and further refined by simulating values in Excel to closely align the experimental TG and DTG curves with the model predictions across the selected heating rates.

The error of the Kambala and Ayous for the five heating rates is shown in the Table 6.

The energy values for Kambala and Ayous, as presented in Tables 3 and 4, were relatively close to each other and aligned with the values reported in the literature. For solid A_1, the activation energies obtained were to the order of 124 and 130 kJ.mol^{-1} for Kambala and Ayous, respectively, compared with the 106 kJ.mol^{-1} reported by Grioui et al. [9]. For solid A_2, the activation energies were 75 kJ.mol^{-1} for Kambala and 87 kJ.mol^{-1} for Ayous, compared with the 107 kJ.mol^{-1} reported by Grioui et al. [9]. For solid A_3, the activation energies were 170 kJ.mol^{-1} for Kambala and 162 kJ.mol^{-1} for Ayous, consistent with Grioui et al.'s value of 170 kJ.mol$-^1$ [9]. The facts that the biomasses studied were different and the tests in this article were performed in dynamic conditions explain the differences observed with Grioui results. Neverthless, they were to the same order of magnitude.

4. Conclusions

The thermal degradation of Kambala and Ayous was investigated through dynamic and isothermal thermogravimetric analysis at five distinct heating rates (3, 5, 7, 10, and 20 K/min). The TG and DTG curves revealed distinct behaviors between Kambala and Ayous, with Kambala displaying a unique profile compared with Ayous and many species reported in the literature. It is noteworthy that the peak typically associated with hemicellulose degradation was absent in the DTG curves for Kambala. Furthermore, two discrete peaks were observed at approximately 500 °C and 700 °C. These were observed for Kambala, corresponding to the degradation of ash. Water washing to remove metals corresponding to the degradation of ash had an impact on the removal of some metals, particularly potassium, whose quantity was reduced by a factor of three. This led to a shift in the TG and DTG curves toward higher temperatures.

The kinetic parameters, namely the activation energies, aligned well with those found in the literature. The degradation model for Kambala was based on four stages, while that of Ayous followed a three-stage model. These results indicate that the models accurately predicted the thermal degradation of both species. Moreover, the findings suggest that this approach can be successfully applied to other tropical wood species by using either a three- or four stage degradation model.

Author Contributions: Conceptualization, Y.R.; methodology, P.G.; software, P.G.; validation, Y.R., P.G. and T.A.-B.; formal analysis, M.C.A.A.; investigation, M.C.A.A.; data curation, P.G.; writing—original draft preparation, M.C.A.A.; writing—review and editing, M.C.A.A., P.G.; vi-

References

1. Cadile, C. Modélisation DEM et Approche Expérimentale de la Dynamique d'un Système Réactifs en Lit Fluidisé Dense: Application à la Gazéification de la Biomasse. Ph.D. Thesis, Université de Toulouse, Toulouse, France, 2014.
2. Girard, P.; Pinta, F.; Van de steene, L. Valorisation énergétique des sous-produits de scieries. *Bois & Forêts des tropiques.* **2003**, *277*, 3.
3. Aubréville, A. Fiche botaniques forestières, industrielles et commerciales: Iroko. *Bois & Forêts des Tropiques* **1947**, *1*, 34–47. [CrossRef]
4. Vernay, M. Un exemple d'utilisation de l'ayous (*Triplochiton scleroxylon*) dans la construction. *Bois & Forêts des Tropiques.* **2005**, *284*, 2.
5. Rogaume, Y. La combustion du bois et de la biomasse. *Rev. Energ. Renouvelables* **2009**, *12*, 123–134.
6. Koufopanos, C.A.; Lucchesi, A.; Maschio, G. Kinetic modelling of the pyrolysis of biomass and biomass components. *Can. J. Chem. Eng.* **1989**, *67*, 75–84. [CrossRef]
7. Batiot, B. Étude et Modélisation de la Cinétique de Décomposition Thermique des Matériaux Solides: Application à la Dégradation du Bois en Cas d'Incendie. Ph.D. Thesis, Université de Poitiers, Poitiers, France, 2014.
8. Goldstein, I.S. (Ed.) *Wood Technology: Chemical Aspects. North Carolina State University*; American Chemical Society: Washington, DC, USA, 1977; p. 43. [CrossRef]
9. Grioui, N.; Halouani, K.; Zoulalian, A.; Halouani, F. Thermogravimetric analysis and kinetics modeling of isothermal carbonization of olive wood in inert atmosphere. *Thermochim. Acta.* **2006**, *440*, 23–30. [CrossRef]
10. Koufopanos, C.A.; Papayannakos, N.; Maschio, G.; Lucchesi, A. Modelling of the pyrolysis of biomass particles. Studies on kinetics, thermal and heat transfer effects. *Can. J. Chem. Eng.* **1991**, *69*, 907–915. [CrossRef]
11. Martí-Rosselló, T.; Li, J.; Leo, L. Kinetic models for biomass pyrolysis. *Arch. Ind. Biotechnol.* **2016**, *1*, 4–7.
12. Prakash, N.; Karunanithi, T. Kinetic modeling in biomass pyrolysis. *J. Appl. Sci. Res.* **2008**, *4*, 1627–1636.
13. Di Blasi, C. Modeling chemical and physical processes of wood and biomass pyrolysis. *Prog. Energy Combust. Sci.* **2008**, *34*, 47–90. [CrossRef]
14. Fan, L.T.; Fan, L.-S.; Miyanami, K.; Chen, T.Y.; Walawender, W.P. A mathematical model for pyrolysis of a solid particle: Effects of the lewis number. *Can. J. Chem. Eng.* **1977**, *55*, 47–53. [CrossRef]
15. Branca, C.; Di Blasi, C. Kinetics of the isothermal degradation of wood in the temperature range 528–708 K. *J. Anal. Appl. Pyrolysis* **2003**, *67*, 207–219. [CrossRef]
16. Thurner, F.; Uzi, M.; Beck, S.R. *Kinectic Investigation of Wood Pyrolysis*; Technical Report; Texas Tech University: Lubbock, TX, USA, 1980.
17. Shen, D.K.; Fang, M.X.; Lu, Z.Y.; Cen, K.F. Modeling pyrolysis of wet wood under external heat flux. *Fire Saf. J.* **2007**, *42*, 210–217. [CrossRef]
18. Shafizadeh, F.; Chin, P.P.S. *Thermal Deterioration of Wood*; American Chemical Society: Washington, DC, USA, 1977; pp. 57–81.
19. Chan, W.-C.R.; Kelbon, M.; Krieger, B.B. Modelling and experimental verification of physical and chemical processes during pyrolysis of a large biomass particle. *Fuel* **1985**, *64*, 1505–1513. [CrossRef]
20. Di Blasi, C. Influences of physical properties on biomass devolatilization characteristics. *Fuel* **1997**, *76*, 957–964. [CrossRef]
21. Várhegyi, G.; Antal, M.J.; Jakab, E.; Szabó, P. Kinetic modeling of biomass pyrolysis. *J. Anal. Appl. Pyrolysis* **1997**, *42*, 73–87. [CrossRef]
22. Wang, W.; Lemaire, R.; Bensakhria, A.; Luart, D. Review on the catalytic effects of alkali and alkaline earth metals (AAEMs) including sodium, potassium, calcium and magnesium on the pyrolysis of lignocellulosic biomass and on the co-pyrolysis of coal with biomass. *J. Anal. Appl. Pyrolysis* **2022**, *163*, 105479. [CrossRef]
23. Müller-Hagedorn, M.; Bockhorn, H.; Krebs, L.; Müller, U. A comparative kinetic study on the pyrolysis of three different wood species. *J. Anal. Appl. Pyrolysis* **2003**, *68*, 231–249. [CrossRef]
24. *ISO 29541:2010*; Solid Mineral Fuels—Determination of Total Carbon, Hydrogen and Nitrogen Content—Instrumental Method. International Organization for Standardization: Geneva, Switzerland, 2010.
25. *ISO 11885:2007*; Dosage d'Eléments Choisis par Spectroscopie d'Emission Optique avec Plasma Induit par Haute Fréquence (ICP-OES). International Organization for Standardization: Geneva, Switzerland, 2007.
26. Chandrasekaran, S.R.; Hopke, P.K.; Rector, L.; Allen, G.; Lin, L. Chemical composition of wood chips and wood pellets. *Energy Fuels* **2012**, *26*, 4932–4937. [CrossRef]

27. El-Sayed, S.A.; Khairy, M. Effect of heating rate on the chemical kinetics of different biomass pyrolysis materials. *Biofuels* **2015**, *6*, 157–170. [CrossRef]

28. Haykiri-Acma, H.; Yaman, S.; Kucukbayrak, S. Effect of heating rate on the pyrolysis yields of rapeseed. *Renew. Energy* **2006**, *31*, 803–810. [CrossRef]

29. Li, A.; Liu, H.-L.; Wang, H.; Xu, H.-B.; Jin, L.-F.; Liu, J.-L.; Hu, J.-H. Effect of heating rate on the pyrolysis yields of rapeseed. *Bio Resour.* **2016**, *11*, 3259–3274.

30. Collard, F.X.; Blin, J. A review on pyrolysis of biomass constituents: Mechanisms and composition of the products obtained from the conversion of cellulose, hemicelluloses and lignin. *Renew. Sustain. Energy Rev.* **2014**, *38*, 594–608. [CrossRef]

31. Williams, P.; Besler, S. The influence of temperature and heating rate on the slow pyrolysis of biomass. *Renew. Energy* **1996**, *3*, 233–250. [CrossRef]

32. Puri, L.; Hu, Y.; Naterer, G. Critical review of the role of ash content and composition in biomass pyrolysis. *Front. Fuels* **2024**, *2*, 1378361. [CrossRef]

33. Grønli, M.G.; Várhegyi, G.; Di Blasi, C. Thermogravimetric analysis and devolatilization kinetics of wood. *Ind. Eng. Chem. Res.* **2002**, *41*, 4201–4208. [CrossRef]

34. Deng, L.; Ye, J.; Jin, X.; Che, D. Transformation and release of potassium during fixed-bed pyrolysis of biomass. *J. Energy Inst.* **2018**, *91*, 630–637. [CrossRef]

35. Nowakowski, D.; Jones, J.; Brydson, R.; Ross, A. Potassium catalysis in the pyrolysis behavior of short rotation willow coppice. *Fuel* **2007**, *86*, 2389–2402. [CrossRef]